



---

## **Dose Distribution in 3D Water Phantom and Profiler 2 Scanning System**

Mpho Enoch Sithole<sup>a\*</sup>, Kabelo McDonald Moji<sup>b</sup>

<sup>a</sup>*Department of Physics, Sefako Makgatho Health Sciences University, Pretoria 0204, South Africa*

<sup>b</sup>*Department of Radiation Oncology, Tshepong Hospital Complex, Klerksdorp 2570, South Africa*

<sup>a</sup>*Email: enoch.sithole@smu.ac.za*

<sup>b</sup>*Email: kmoji@nwpg.gov.za*

### **Abstract**

In commissioning of medical linear accelerator 3D water phantom is used. The procedure required a lot of efforts and is time consuming. The purpose of the study is to determine whether a Profiler 2 scanning system can be used as a substitute for 3D water phantom. All the measurements were performed with 6 and 15 MV photon beams generated by Elekta Synergy linear accelerator. Percentage depth dose and beam profiles were measured for 6×6, 10×10, 14×14, 20×20, and 25×25 cm<sup>2</sup> field sizes defined at 0.5, 1.0, 2.0, and 5.0 cm. Dose distributions compared well within recommended limits, with the largest difference, in symmetry of 1.6%, flatness of 2.47%, penumbra of -12.11 mm, which was just outside the recommended limit of 12 mm, field size of 3.39 mm, and PDD<sub>10</sub> of 1.69%. The results showed the suitability of the profiler 2 scanning system to be used for commissioning of linear accelerators.

**Keywords:** Water phantom; Profiler 2 scanning system; photon beam; dose distribution.

### **1. Introduction**

Since the introduction of linear accelerators in the department of radiotherapy, commissioning has always been the most important part of beam data measurements to be done before the machine can be used for clinical purposes.

---

\* Corresponding author.

In radiotherapy one often needs to compare two dose distributions, especially with the wide clinical implementation of the Intensity Modulated Radiation Therapy (IMRT) and software tools for quantitative dose (or fluence) distribution comparison which are required for patient-specific quality assurance. Dose distribution comparison is not a trivial task since it has to be performed in both dose and spatial domains in order to be clinically relevant. Each of the existing comparison methods has its own strengths and weaknesses and there is a room for improvement [1]. There are different methods or tools developed to quantitatively compare dose distributions, either measured or calculated. Before computing gamma index ( $\gamma$ ), the dose and distance scales of the two distributions, referred to as evaluated and reference, are normalized by dose and distance criteria. The renormalization allows for dose distribution comparison to be conducted simultaneously along dose and distance axes. In typical clinical use, the fraction of points that exceeds 3% and 3 mm can be extensive, thus typical a 5% and 2-3 mm is used in clinical evaluation [2, 3].

Modern radiation therapy has advanced considerably in the recent decades through the development of conformal techniques that better shape the high dose to tumor volumes while minimizing the dose to the surrounding normal tissue. The rapid pace of these developments and significant increase in the associated complexities, have introduced considerable new challenges to the radiation treatment team. The challenges for patient treatment verification have motivated the development increasingly sophisticated strategies, tools and equipments to measure dose and to analyse the measurements so that physicists can assess safe delivery of dose to patients. Point dosimeters such as ionization chambers, thermoluminescent dosimeters and diodes have been used for decades to commission treatment units, to calibrate output and to verify dose delivery at single points in a phantom.

The 2D dosimetry techniques such as silver-halide and radiochromic film or digital systems incorporating flat panel arrays of ionization chambers or diodes that are often used in IMRT delivery validation, and the full 3D dosimeters such as scintillation detector array or volumetric chemical dosimeters probed by Magnetic Resonance Imaging (MRI) or by radiographic examination and optical computed tomography (CT) techniques for IMRT (Intensity Modulated Radiation Therapy) and VMAT (Volumetric Modulated Arch Therapy) has also been used [4, 5]. Advances in computer technology have led to the availability of sophisticated 3D treatment planning systems (TPSs) for use in many radiotherapy centers. The aim of introducing such TPSs is to improve the accuracy of dose calculations in radiotherapy planning [6]. Many optimization functions and methods, including gradient methods and stochastic optimization methods, to solve dose distribution problems in radiotherapy planning have been used [6, 7].

Two types of cost functions, deterministic models that are based on radiobiological effects or dose criteria and probability models that are similar to the maximum likelihood estimations have been successfully applied to radiotherapy planning [8]. Dose distributions can also be compared both statistically and graphically. Graphs aid in statistical analysis of the distributions, as well as both cross-plots and depth-doses, is provided by STATDOSE [9]. Although in our study the algorithms within the TPS (CMS XiO) as well as excel generated data will be used for data analysis. The CMS XiO 3D-TPS system is based on the pencil beam model, where physical quantities such as profiles and percentage depth dose curves are estimated using conventional method. The photon dose calculation model in this TPS system is based on convolution, superposition and Clarkson's

algorithms [10]. The mono-energetic depth doses, calculated with convolution method from Monte Carlo generated point spread functions (PSF), are added to yield the pure photon depth dose distributions [3]. The obtained poly-energetic pencil-beam is then used to calculate the dose distribution for a given case by convolution with the machine specific energy-fluence matrix modulated by the actual field shape. One of the features of the system is that it calculates the monitor settings for the planned fields [3]. The purpose of this study was to determine and compare the beam profile for the profiler 2 scanning system to be used as a substitute for 3D water phantom during linear accelerator commissioning.

## **2. Materials and methods**

### **2.1. 3D-Water phantom**

Setting up the water phantom system properly can help improve the workflow, and more importantly, reduce the collection of suboptimal data, which may result in considerable amount of processing and sometimes may even require rescanning. Before setting up the water phantom for data collection, a periodic quality assurance was performed as outline by Das and his colleagues (2008) [11]. The two ion-chambers were used for scanning a field chamber that moves in the tank as programmed and a reference chamber, which is stationary in the field. The reference chamber was used to remove the instantaneous fluctuations in the incident beam output. The 3D-water phantom was setup under the linear accelerator for measurements of the photon (6 and 15 MV) beam data. The acquisition plans were setup on a scanning computer using the real time dosimetry (RTD) multidata scanning software for both the 6 and 15 MV photon beams. Dose distribution data was collected for the defined field sizes; 6×6, 10×10, 14×14, 20×20, and 25×25 cm<sup>2</sup>, all defined at the depths of 0.5, 1.0, 2.0, and 5 cm.

### **2.2. Profiler 2 scanning system**

The profiler 2 scanning system was calibrated properly for both array and dose calibration before it could be used. The system was stored in the treatment room for at least 30 minutes to allow for all parts of the instrument to reach the temperature equilibrium [12]. Perspex slabs were added on top of the profiler 2 scanning system to simulate the depths. The source-surface distance (SSD) was kept constant at 100 cm throughout the measurements. The same field sizes and depths scanned in a 3D-water phantom were scanned in a profiler 2 scanning system for the same beam energies. The profiler 2 scanning system is designed to measure beam profiles rather than depth doses, therefore the 0.6 cm<sup>3</sup> farmer type ion chamber was inserted in a calibration block (Perspex block) with dimensions 4.4 cm and 0.6 cm [13].

### **2.3. Beam modelling**

Following the collection of scanned data, it was necessary to do some processing before sending data to the treatment planning system for modelling. The amount of processing depends on the type of the scanner, the accuracy of setup, and characteristics of the machine itself [14, 15]. All measured data have a varying degree of noise depending on the system. Smoothing and filtering routines were used to remove noise and extract actual data. Only the 10×10 cm<sup>2</sup> beam data were exported to CMS XiO treatment planning system (TPS) for modelling and for the purpose of validation.

### 3. Results

The following figures present the beam profiles and percentage depth doses (PDDs) acquired in 3D-water phantom and Profiler 2 scanning system for the 6 and 15 MV photon beams. Each beam profile was normalized differently for presentation, i.e. 100, 95, 90, 85, and 80% for field sizes 6×6, 10×10, 14×14, 20×20, and 25×25 cm<sup>2</sup> respectively. An accurate dose measured in phantom requires an accurate description of the radiation source [16]. Before data can be reliably used as input for dose measurement, it must be properly validated. Table 1 shows the photon beam properties for 6 and 15 MV measured in water phantom for 10×10 cm<sup>2</sup> field size defined at SSD of 100 cm. The maximum values of gamma ( $\gamma$ ) index obtained were 0.78 and 0.63 for 6 and 15 MV respectively. The values of  $\gamma$  index in all regions were less than 1.0, which are within acceptable level.

**Table 1:** Measured properties of 6, and 15 MV photon beams for 10 × 10 cm<sup>2</sup> field size defined at 100 cm SSD in water phantom.

Energy	D <sub>max</sub> (cm)	D <sub>10</sub> (%)	D <sub>20</sub> (%)	D <sub>20</sub> /D <sub>10</sub>	TPR <sub>20,10</sub>	R <sub>50</sub> (cm)
6 MV	1.5	67.65	38.63	0.572	0.665	15.5
15 MV	3.0	75.97	49.85	0.656	0.771	19.8

Figure 1 presents the comparison of beam profiles measured in 3D-water phantom and Profiler 2 scanning system for 6 MV photon beam measured for 6×6, 10×10, 14×14, 20×20, and 25×25 cm<sup>2</sup> field sizes, while Fig 2 shows the beam profile measured for 15 MV photon beam. The dose profiles were measured at a depth of maximum dose ( $d_{max}$ ), 1.5 and 3.0 for 6 and 15 MV respectively. All curves were normalized to the maximum dose along the central axis. The shape of the beam profile was found to vary with beam energy more than the shape of the depth dose curves.

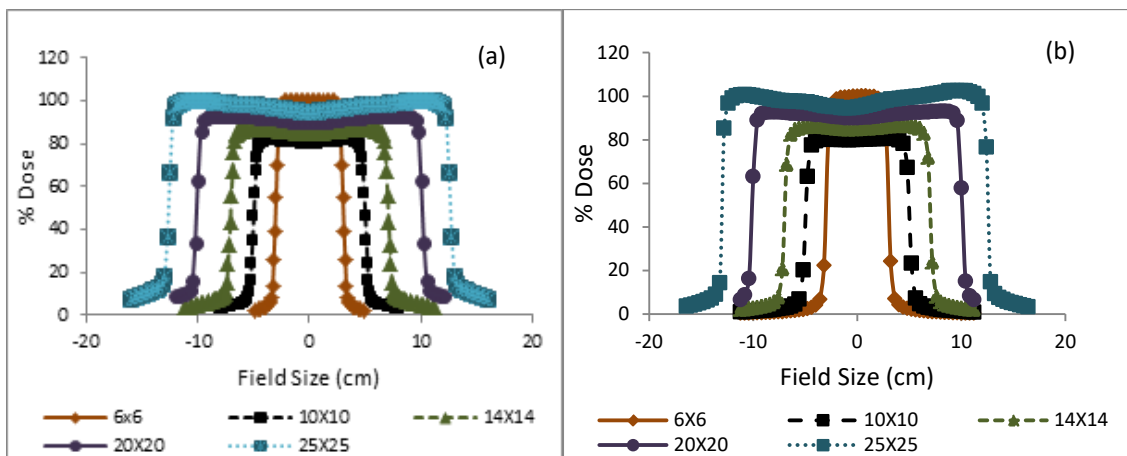


**Figure 1:** Measured beam profiles (a) 3D Water phantom. (b) Profiler 2 scanning system for 6 MV photon beam.

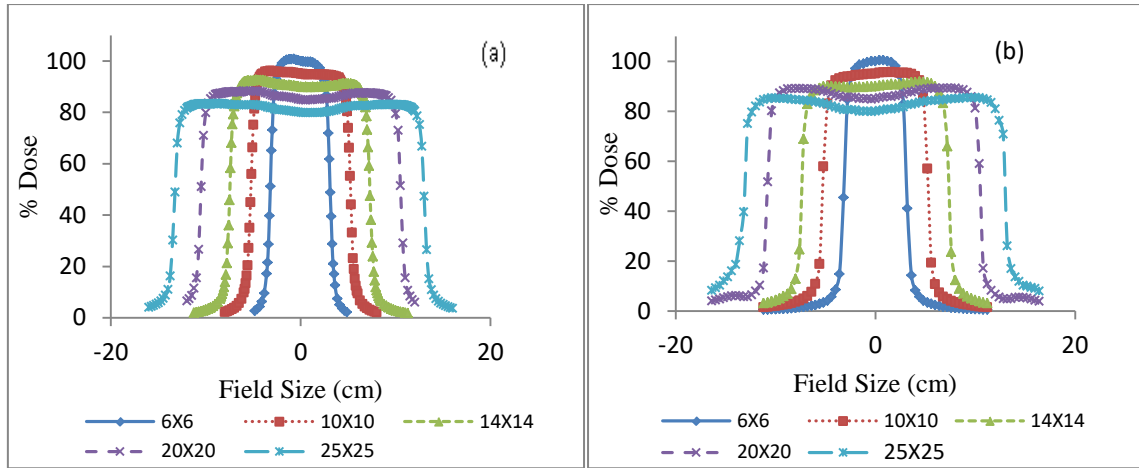


**Figure 2:** Measured beam profile (a) 3D Water phantom. (b) Profiler 2 scanning system for 15 MV photon beam.

Table 2 and 3 present the properties of beam profiles measured in 3D-water phantom and Profiler 2 scanning system for 6 and 15 MV photon beams, respectively.

The beam profiles were measured at 0.5 cm depth for both system. The highest percentage differences were observed for  $25 \times 25 \text{ cm}^2$  in both energies. The notations in table 2 and 3 are defined as follows:

$\Delta_{1,PDD}$  ( $PDD_{10}$ ), is a point on the central beam axis beyond  $d_{max}$  to depth at which dose is 10% of maximum with a limit of 2%.

$\Delta_{2,PDD}$  (Build-up in PDDs), is a point on the central beam axis in the build-up region, also a displacement of isodose curves, with a limit of 2%.

$RW_{50}$ : (Field size), is the difference in radiological width, which is defined as the width of the profile at half its central axis value with a limit of 2 mm for field sizes less than  $20 \times 20 \text{ cm}^2$ .

$F_r$  (Penumbra): difference in the beam fringe or penumbra, which is the distance between the 90% of the maximum and 20% of the maximum points on the profile, with a limit of  $\pm 12 \text{ mm}$ .

$\Delta_3$  (Flatness): the maximum ratio of the maximum absorbed dose (anywhere in the radiation field) to the minimum absorbed dose in the flattened area at the standard measurement depth with a limit of 3%.

$\Delta_4$  (Symmetry): the maximum ratio of the absorbed dose at any two points. Symmetrically displaced about the beam axis and within the flattened area at the standard measurement depth with a limit of 3%.

Figure 3 (a) and (b) show comparison of beam profile data acquired with CMS XiO treatment planning system with profiler 2 scanning system and 3D water phantom for 6 and 15 MV photon beams, respectively. The beam data were measured at 1.0 cm depth for  $10 \times 10 \text{ cm}^2$  field size. Data for all three systems were superimposed.

Figure 4 (a) and (b) show comparison of PDDs data acquired with CMS XiO treatment planning system with profiler 2 scanning system and 3D water phantom for 6 and 15 MV photon beams, respectively. The beam data were measured for  $10 \times 10 \text{ cm}^2$  field size.

**Table 2:** Comparison of beam profiles for the 6 MV photon beam measured at 0.5 cm depth.

FS (cm)	3DWater Phantom				Profiler 2Scanning				Differ			
	$\Delta_4$ (%)	$\Delta_3$ (%)	$F_r$ (cm)	$RW_{50}$ (cm)	$\Delta_4$ (%)	$\Delta_3$ (%)	$F_r$ (cm)	$RW_{50}$ (cm)	$\Delta_4$ (%)	$\Delta_3$ (%)	$F_r$ (cm)	$RW_{50}$ (cm)
6x6	0	0.33	0.43	0.06	0.3	1.3	0.40	0.05	0.3	0.97	-	0.01
												0.03
10x10	0	1.48	0.48	0.10	0.3	0.8	0.41	-0.06	0.3	-	-	0.04
14x14	0	2.43	0.51	0.21	0.3	2.2	0.41	-0.11	0.3	0.68	0.07	0.10
20x20	0	3.48	0.59	0.29	0.3	3.7	0.32	-0.10	0.3	-0.23	-	0.19
25x25	0	5.43	0.61	0.27	1.6	7.7	0.28	0.16	1.6	0.22	0.10	0.11
										2.27	-	
												0.27
												-
												0.33

**Table 3:** Comparison of beam profiles for the 15 MV photon beam measured at 0.5 cm depth.

FS (cm)	3DWater Phantom				Profiler 2Scanning				Differ			
	$\Delta_4$ (%)	$\Delta_3$ (%)	$F_r$ (cm)	$RW_{50}$ (cm)	$\Delta_4$ (%)	$\Delta_3$ (%)	$F_r$ (cm)	$RW_{50}$ (cm)	$\Delta_4$ (%)	$\Delta_3$ (%)	$F_r$ (cm)	$RW_{50}$ (cm)
6x6	0	0.72	0.46	0.07	1.3	0.7	0.44	-0.04	1.3	-	-	0.03
										0.02	0.02	
10x10	0	1.41	0.53	0.15	1.5	1.7	0.43	-0.03	1.5	0.29	-	0.12
14x14	0	3.65	0.71	0.31	1.5	3.5	0.46	-0.01	1.5	-	0.10	0.30
20x20	0	5.9	1.16	0.40	1.5	4.9	0.43	-0.06	1.5	0.15	-	0.34
25x25	0	7.13	1.15	0.37	0.5	9.6	0.30	0.17	0.5	-	0.25	0.20
										1.00	-	
										2.47	0.73	
												-
												1.21

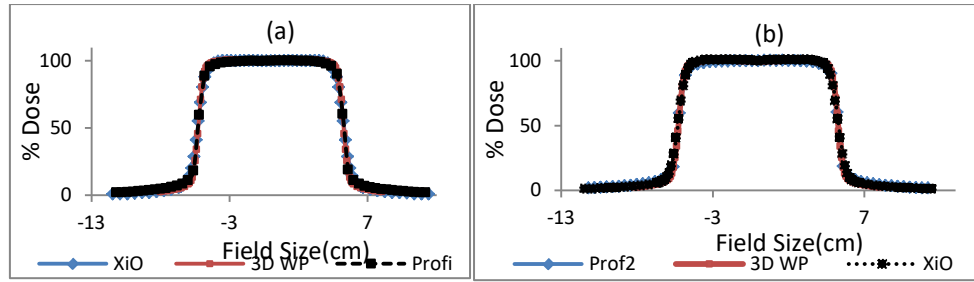


**Figure 3:** Comparison of the 3D Water phantom, Profiler 2 scanning system, and XiO beam profiles for the  $10 \times 10 \text{ cm}^2$  field size for (a) 6 MV and (b) 15 MV photon beams.

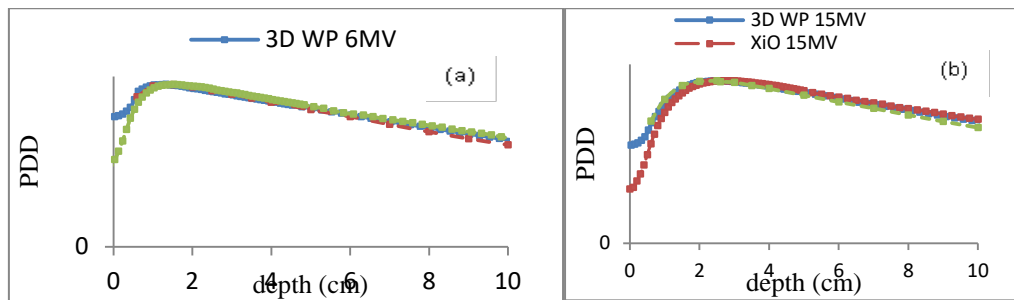


**Figure 4:** Comparison of PDDs the 3D Water phantom, Profiler 2 scanning system, and XiO beam profiles for the  $10 \times 10 \text{ cm}^2$  field size for (a) 6 MV and (b) 15 MV photon beams.

#### 4. Discussion

Table 1 shows the photon beam properties for 6 and 15 MV measured in water phantom for  $10 \times 10 \text{ cm}^2$  field size defined at SSD of 100 cm. Maximum values of gamma index ( $\gamma$ ) for  $10 \times 10 \text{ cm}^2$  field size at the maximum dose ( $d_{\text{max}}$ ) were 0.78 and 0.63 for 6 and 15 MV photon beams, respectively. The values of  $\gamma$  index at other specific points were less than 1.0, which indicates that the measured data has passed the acceptance test. The results are in agreement with the work published by Ding and Ding (2012) [17]. From Figures 1 and 2, it was evident that there was a slight difference between the 3D-water phantom and profiler 2 scanning system which were well within the acceptable limits. The differences in the horn area (area of high dose) were within 2 mm (+/-2%), the penumbra region (edges of the beam) were also well within 2 mm (+/2%), as well as in the washout area (area of dose variation as a result of both leakage and scatter from the collimator system). Elder and his colleagues (1995) [10] found an agreement to within 1.5% for the ionization chamber measurements and the solid state detector beam profiles, whilst Leavitt and Klean (1997) [18] has found a maximum difference of 2.7%. From tables 2 and 3, the maximum difference in symmetry was 1.6% for a 6 MV photon beam for the  $25 \times 25 \text{ cm}^2$  field size, and 1.5% for a 15 MV photon beam for field sizes ( $10 \times 10 \text{ cm}^2$ ,  $14 \times 14 \text{ cm}^2$ , and  $20 \times 20 \text{ cm}^2$ ). The maximum difference in flatness was 2.27% for 6 MV photon beam for a  $25 \times 25 \text{ cm}^2$  field size, and 2.47% for a 15 MV photon beam for a  $25 \times 25 \text{ cm}^2$  field size, which were within the recommended limit of +/- 3%. The penumbra maximum difference measured was -0.334 cm for a 6 MV photon beam for a  $25 \times 25 \text{ cm}^2$ , and the 15 MV photon beam was -1.211 cm for a  $25 \times 25 \text{ cm}^2$  which was just outside the recommended limit of 1.2 cm and this can be due to insufficient scatter contribution due to the size of the profiler 2 scanning system,

with a field size maximum difference of 0.187 cm for a 6 MV photon beam for a 20×20 cm<sup>2</sup>, and 0.339 cm for 15 MV photon beam for a 20×20 cm<sup>2</sup> which were within the recommended limit of 0.2 cm for smaller field sizes than 20×20 cm<sup>2</sup> and 0.4 cm for larger field sizes. It is evident that the 6 MV photon beam flatness for the field sizes 20×20, and 25×25 cm<sup>2</sup> needed to be adjusted, same as for the 15 MV photon beam, the flatness of the field sizes 14×14, 20×20, and 25×25 cm<sup>2</sup>. It is evident from Figure 3 that the comparison between the 3D water phantom, profiler 2 scanning and CMS XiO beam profiles for both 6 and 15 MV photon beams was in agreement, within 1 mm ( $\pm 1\%$ ) with the limit of 3 mm ( $\pm 3\%$ ) as recommended by CMS XiO for the 10×10 cm<sup>2</sup> field sizes measured at 5.0 cm depth [19]. Figures 4(a) and (b), showed the results for both the 6 and 15 MV PDDs for the 3D-water phantom, Perspex block and CMS XiO. It can be deduced that comparison was very well within recommended limit, especially at the depth of  $d_{max}$ . The deviation was observed to be outside the recommended limit at the build-up region as well as the depth larger than 5 cm with the Perspex block. This simply meant that the Perspex block cannot be used to substitute the 3D water phantom for PDD measurements during the commissioning of a linear accelerator. The Perspex block can only be used as a rough estimation for energy checks in quality assurance measurements. There is fewer limitation of profiler 2 scanning system. There is a buildup region of PDDs for the Perspex slabs. This was due to the inherent build up in the Perspex, which restricts for measurements to be taken at the surface. Thus it will be difficult to predict the surface dose using Perspex slabs. The other limitations with the Perspex slabs was the number of Perspex slabs to be used to measure PDDs at depths deeper than 10 cm and the measurements of diagonal profiles.

## **5. Conclusion**

In general, this work provided the comparison between the 3D-water phantom and the profiler 2 scanning system. The ionization chambers gave accurate results as expected, but the data acquisition was very time consuming, thus the array diode detectors showed in general a good reasonable agreement with the ionization chambers measurements. From the measurements performed and results achieved, it showed that the profiler 2 scanning system can be used for commissioning of the linear accelerator. The profiler 2 scanning system needs to be properly calibrated for linear array diode detectors and dose. The calibration factors will be necessary for measurements of both profiles and dose. Dose distribution measured with the profiler 2 scanning system is recommended for centers that wish to commission a linear accelerator similar to the one already on site so that beam matching of the accelerator can be assumed.

## **Acknowledgements**

The authors would like to thank the Klerkdorp-Tshepong hospital complex for the support and permission to use and utilize their facilities.

## **References**

- [1]. S.B. Jiang, G.C. Sharp, T. Neicu, R.I. Berbeco, et al. "On dose distribution comparison." *Physics in Medicine and Biology*, vol. 51, pp. 759-762, 2006.
- [2]. D.A. Low and J.F. Dempsey. "Evaluation of the gamma dose distribution comparison method."



American Association of Physicists in Medicine, 2003.

- [3]. E. Amin, and H.M. Meir. "Verification of Photon Beam Data Calculated by a Treatment Planning System Based on Pencil Beam Model." *Journal of the Egyptian Nat. Cancer Institute.* vol. 13, pp. 57-62, 2001.
- [4]. L.J. Schreiner. *On the quality assurance and verification of modern radiation therapy treatment* Department of Oncology and Physics. Queen's University, Kingston, Ontario: Canada, 2011, pp. 189-191.
- [5]. A. Fogliata, G. Nicolini, M. Alber, et al. "On the performances of different IMRT treatment planning systems for selected paediatric cases" *Oncology Institute of Southern Switzerland, Medical Physics.* pp. 1-21, 2007.
- [6]. ICRU. *Use of Computers in External Beam Radiotherapy Procedures with High Energy photons and Electrons.* International Commission on Radiation Units and Measurements. 1987, pp. 424-446.
- [7]. X. Wu and Y. Zhu. "A maximum entropy method for the planning of conformal radiotherapy." *Medical Physics.* vol. 3, pp. 2241-2246, 2001.
- [8]. L. Xing, J.G. Li, A. Pugacher, Q.T. Le, et al. "Estimation theory and model parameter selection for therapeutic treatment plan optimization." *Medical Physics.* vol. 26, pp. 2348-2358, 1999.
- [9]. H.C.E. McGowan, B.A. Faddegon and C.M. Ma. *STATDOSE for 3D dose distributions.* Ionization Radiation Standards, 2007, NRCC 1-10.
- [10]. P.J. Elder, F.M. Coveney and A.D. Welsh. "An investigation into comparison between different dosimetric methods of measuring profiles and depth doses for dynamic wedges on a Varian 600C linear accelerator." *Physics in Medicine and Biology.* vol. 40, pp. 683-689, 1995.
- [11]. J.J. Das, C. Chee-Wai, R.J. Watts, A. Ahnesjo, et al. *Accelerator beam data commissioning equipment and procedure.* Report of the TG-106 of the Therapy Physics Committee of the AAPM, 2008, pp. 4186-4215.
- [12]. R.C. Taylor, C. Chu, D.S. Followill, W.F. Hanson. "Equilibration of air temperature inside the thimble of a farmer-type ion chamber." *Medical Physics.* vol. 25, pp. 496-502, 1998.
- [13]. H. Song, M. Ahmad, J. Deng, et al. "Limitations of silicon diodes for clinical electron dosimetry." *Radiation Protection Dosimetry.* vol. 120, pp. 56-59, 2006.
- [14]. O.A. Ali, C.A. Willemse, W. Shaw, F.C.P. du Plessis, et al. "Monte Carlo electron source model validation for an Elekta Precise linac." *Medical Physics.* vol. 38, pp. 2366-2373, 2011.
- [15]. J. Shi, W.E. Simon and T.C. Shu. "Modelling the instantaneous dose rate dependence of radiation diode detectors." *Medical Physics.* vol. 30, pp. 2509-2519, 2003.
- [16]. D. Sheikh-Bagheri and D.W.O. Rogers. "Monte Carlo simulation of nine megavoltage photon beam spectra using beam code." *Medical Physics.* vol. 29, pp. 391-402, 2002.
- [17]. G.X. Ding and F. Ding. "Beam characteristics and stopping-power ratios of small radiosurgery photon beams." *Physics in Medicine and Biology.* vol. 57, pp. 5509-5521, 2012.
- [18]. D.D. Leavitt and E. Klein. "Dosimetry measurement tools for commissioning enhanced dynamic wedge." *Medical Dosimetry.* vol. 22, pp. 171-176, 1997.
- [19]. TRS-398. *Absorbed dose determination in external beam radiotherapy. An international code of practice for dosimetry based on standards of absorbed dose to water,* IAEA, 2001.